THE JOURNAL OF BIOLOGICAL CHEMISTRY VOL. 287, NO. 17, pp. 14109–14121, April 20, 2012

A Single Amino Acid Substitution in IIIf Subfamily of Basic Helix-Loop-Helix Transcription Factor AtMYC1 Leads to Trichome and Root Hair Patterning Defects by Abolishing Its Interaction with Partner Proteins in *Arabidopsis*[*]

Received for publication, July 8, 2011, and in revised form, February 13, 2012 Published, JBC Papers in Press, February 14, 2012, DOI 10.1074/jbc.M111.280735

Hongtao Zhao[‡§], **Xiaoxue Wang**[¶], **Dandan Zhu**[‡], **Sujuan Cui**[‡], **Xia Li**[§], **Ying Cao**[‡], **and Ligeng Ma**[‡‖1]

From the [‡]*Hebei Key Laboratory of Molecular Cell Biology, College of Biological Sciences, Hebei Normal University, Shijiazhuang 050016, Hebei, China,* [‖]*College of Life Science, Capital Normal University, Beijing 100048, China,* [§]*State Key Laboratory of Plant Cell and Chromosome Engineering, Center of Agricultural Resources, Institute of Genetics and Developmental Biology, Chinese Academy of Sciences, Shijiazhuang, Hebei 050021, China and* [¶]*National Institute of Biological Sciences, Beijing 102206, China*

Background: IIIf subfamily of bHLH members GL3/EGL3 involved in epidermal cell fate determination through interacting with MYBs/TTG1.
Results: A substitution of R173H in the AtMYC1 homolog of GL3/EGL3 abolished its function in trichome and non-hair cell fate control.
Conclusion: The functionally conserved Arg residue in AtMYC1/GL3/EGL3 was crucial for protein interaction and proper biological function.
Significance: A novel critical and functionally conserved site in IIIf bHLH proteins was identified.

Plant trichomes and root hairs are powerful models for the study of cell fate determination. In *Arabidopsis thaliana*, trichome and root hair initiation requires a combination of three groups of proteins, including the WD40 repeat protein TRANSPARENT TESTA GLABRA1 (TTG1), R2R3 repeat MYB protein GLABRA1 (GL1), or WEREWOLF (WER) and the IIIf subfamily of basic helix-loop-helix (bHLH) protein GLABRA3 (GL3) or ENHANCER OF GLABRA3 (EGL3). The bHLH component acts as a docking site for TTG1 and MYB proteins. Here, we isolated a mutant showing defects in trichome and root hair patterning that carried a point mutation (R173H) in *AtMYC1* that encodes the fourth member of IIIf bHLH family protein. Genetic analysis revealed partial redundant yet distinct function between *AtMYC1* and *GL3*/*EGL3*. *GLABRA2* (*GL2*), an important transcription factor involved in trichome and root hair control, was down-regulated in *Atmyc1* plants, suggesting the requirement of *AtMYC1* for appropriate *GL2* transcription. Like its homologs, AtMYC1 formed a complex with TTG1 and MYB proteins but did not dimerized. In addition, the interaction of AtMYC1 with MYB proteins and TTG1 was abrogated by the R173H substitution in *Atmyc1-1*. We found that this amino acid (Arg) is conserved in the AtMYC1 homologs GL3/EGL3 and that it is essential for their interaction with MYB proteins and for their proper functions. Our findings indicate that AtMYC1 is an important regulator of trichome and root hair initiation, and they reveal a novel amino acid necessary for protein-protein interactions and gene function in IIIf subfamily bHLH transcription factors.

Plant trichomes and root hairs are derived from epidermal cells in above- and under-ground tissues, respectively. Whereas trichomes protect plants from UV radiation, wind, frost, and insects (1, 2), root hairs enhance water and nutrient absorption, help anchor plants to the soil, and facilitate communication with biotic and abiotic factors in the soil (3). For biologists, the differentiation and morphogenesis of trichomes and root hairs from initially equivalent cells have provided an important insight into cell fate determination (2–4). In *Arabidopsis* roots, epidermal cells differentiate in a position-dependent manner (5–9). Epidermal cells in contact with two cortical cells develop into hair cells, whereas epidermal cells in contact with one cortical cell become non-hair cells (2, 3).

Unlike their root counterparts, trichomes are distributed on the rosette leaves, the stem, cauline leaves, and sepals without any spatial correlation to morphological landmarks (1, 4). However, trichomes are regularly separated and rarely clustered in the wild type, suggesting the existence of a patterning mechanism (10, 11).

Years of genetic and molecular studies have revealed that the cell fate determination of trichomes and root hair cells is controlled by similar molecular mechanisms (2, 3). Three factors, the WD40 repeat protein TRANSPARENT TESTA GLABRA1 (TTG1), R2R3 repeat MYB protein GLABRA1 (GL1; for the trichomes), or WEREWOLF (WER; for the root non-hair cells) and the basic helix-loop-helix (bHLH)[2] protein GLABRA3 (GL3) or ENHANCER OF GLABRA3 (EGL3) constitute an

[*] This work was supported by China MOST 973 Project Grants 2012CB910900 and 2012CB114200 and by the Hebei Province key laboratory program.
[1] To whom correspondence should be addressed: Hebei Key Laboratory of Molecular Cell Biology, College of Biological Sciences, Hebei Normal University, Shijiazhuang 050016, Hebei, China. Tel.: 86-311-86269144; Fax: 86-311-86269300; E-mail: Ligeng.ma@mail.hebtu.edu.cn.

[2] The abbreviations used are: bHLH, basic helix-loop-helix; Col, Columbia; BiFC, bimolecular fluorescence complement; LCR, low complexity regions.

active R2R3 MYB-bHLH-WD40 complex that initiates trichome and non-hair cell differentiation (1, 2, 4, 12–15). *GLABRA2* (*GL2*), a homeodomain transcription factor, is the immediate downstream target of the active complex and is involved in morphological development and maturation of the trichome and non-hair cell (16–20). Mutations in these factors result in fewer or even no trichomes production and/or ectopic root hairs formation.

In contrast, R3 MYB proteins, including CAPRICE (CPC), TRIPTYCHON (TRY), ENHANCER OF TRY AND CPC 1 (ETC1), ETC2, or ETC3/CPL3, act as negative regulators of trichomes initiation and non-hair cells differentiation. Mutations of these factors lead to increased trichome number and/or trichome clusters and reduced root hairs (21–29). These inhibitors are activated by R2R3 MYB-bHLH-WD40 complex in trichomes and non-hair cells and then move quickly to adjacent cells, where they compete with the R2R3 MYB proteins for binding to bHLH proteins; the involvement of R3 MYB proteins creates an inactive complex that inhibits trichome and non-hair cell initiation (25, 26, 29–31).

In the MYB-bHLH-WD40 complex, the WD40 component is encoded by a single-copy gene, *TTG1*. WD40 domains generally function in protein-protein interactions, and there is evidence that TTG1 binds to bHLH proteins directly (13, 15, 32). MYB proteins constitute one of the largest transcription factor families in *Arabidopsis* (33). R2R3 repeat MYB proteins, including GL1, MYB23, and WER, regulate trichome and non-hair cell patterning through interacting with bHLH proteins (12, 14, 15, 32, 34). R3 repeat MYB proteins, which do not possess an activation domain (AD), bind to bHLH proteins and thereby interfere with the R2R3-MYB-bHLH-WD40 interaction and render the complex inactive (1, 2, 28, 31, 35).

It has been shown that bHLH proteins serve as a docking site in multiprotein interactions (36). There are roughly 133 members of the bHLH family, making it one of the largest transcription factor superfamilies in *Arabidopsis* (37, 38). A comprehensive analysis classified these genes into 12 subfamilies. Based on the functions of known members of this transcription factor family, it was speculated that different members participate in distinct plant developmental processes (37). Among them, members of the IIIf subgroup, including *GL3*, *EGL3*, and *TT8*, function in trichome initiation, root hair patterning, flavonoid/anthocyanin metabolism, and/or mucilage biosynthesis (12–14, 35, 39–41). This subgroup is homologous to the bHLH transcription factors R and B in *Zea mays*, which also function together with the MYB proteins C1 and Pl to control anthocyanin production (37, 42–43). *AtMYC1*, the fourth member of the R/B-like IIIf subfamily of bHLH transcription factors in *Arabidopsis*, was first cloned by Urao *et al.* in 1996 (44); subsequently it was characterized as the direct target as GL3 by Morohashi and Grotewold (20), and it was shown to interact with GL1 and WER in yeast (45), and after we finished this manuscript, it was reported that AtMYC1 is an important source of variation for trichome cell fate determination in different ecotypes of *Arabidopsis thaliana* (46).

Here, we characterized the function of *AtMYC1* in root hair development in addition to in trichome cell fate determination through the isolation of a mutant carrying a point mutation in *AtMYC1*. We found that the function of *AtMYC1* is partially redundant yet distinct with that of *GL3/EGL3* in trichome and root hair development, probably through the regulation of *GL2* expression. Furthermore, we identified an amino acid residue that is functionally conserved among the R/B-like IIIf subfamily of bHLH transcription factors and which is necessary for the interaction between bHLH and MYB proteins in trichome and root hair patterning.

EXPERIMENTAL PROCEDURES

Plant Materials and Growth Conditions—The *A. thaliana* stocks described in this work were of the Columbia (Col) ecotype. *Atmyc1-2*, *Atmyc1-3*, and *gl3-11* correspond to SALK_056899, SAIL_227_H01, and SALK_118201, respectively. Seeds were surface-sterilized in 75% ethanol, washed with sterile water, kept at 4 °C in a chamber for 2 days, and then planted on Murashige and Skoog medium. After 8 days, the seedlings were transferred to soil and grown in a growth chamber under long-day conditions (16 h of light/8 h of dark) at 65% relative humidity.

Positional Cloning—The *Atmyc1-1* mutant (Col background) was crossed with wild-type Landsberg *erecta* (L*er*) plants. The F2 population was used for mapping. Simple sequence length polymorphism (SSLP), cleaved amplified polymorphic sequence (CAPS), and derived CAPS (dCAPS) markers were designed according to differences announced publicly on the TAIR website (47, 48).

Microscopy—Root hair cell number and cell type pattern analysis were carried on with toluidine blue-stained 4-day-old seedling roots, viewed with differential interference contrast optics. At least 20 seedling roots were analyzed for each strain. Epidermis with visible protrusion was taken as root hair cells (12).

RNA Extraction and Real-time PCR—Total RNA for quantitative real-time PCR was prepared using TRI Reagent Solution (Ambion) according to the manufacturer's handbook. After digestion with RNase-free DNase (Promega) to eliminate contaminating DNA, 3 mg of total RNA were used for reverse transcription (Fermentas). Real-time PCR was carried out using Takara SYBR Premix Ex Taq in a 7500 real-time PCR instrument (Applied Biosystems).

Plasmid Construction and Plant Transformation—To construct *pAtMYC1*::*AtMYC1* for our complementation analysis, a 2581-bp 5′-regulatory sequence together with the coding sequence of *AtMYC1* was inserted into the binary vector *pCAMBIA1300* and introduced into *Atmyc1-1* by *Agrobacterium tumefaciens*-mediated floral transformation (49). To construct *pAtMYC1::GUS*, the above promoter was inserted upstream of *GUS* in the *pCAMBIA 1300*, and the construct was transformed into wild-type plants.

GUS Staining—GUS staining was performed as described by Cao *et al.* (50). Trichome staining in mature leaves was done using T1 plants; all other tissues were taken from T3 plants.

Scanning Electron Microscopy—Fresh 10-day-old seedlings were fixed in 50% ethanol, 5% acetic acid, and 3.7% formaldehyde overnight at 4 °C then dehydrated in an ethanol series (once in 30, 50, 70, and 95% and twice in 100%). The samples were then freeze-dried overnight in tertiary butyl alcohol. The

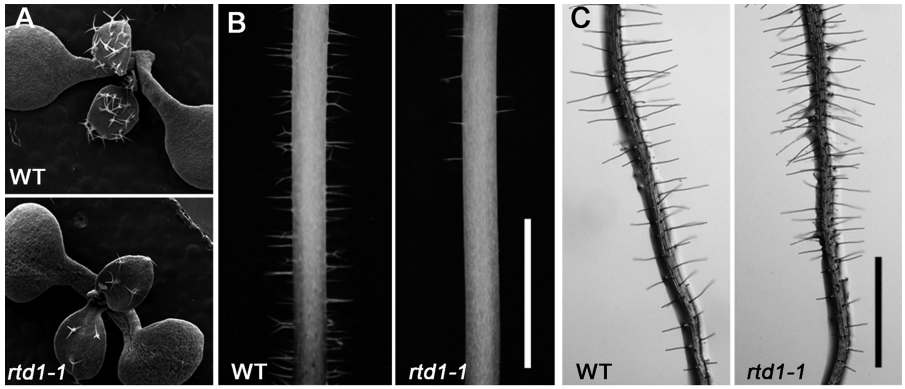

FIGURE 1. **Isolation of a mutant with reduced trichomes and increased root hairs.** *A*, shown are scanning electron micrographs of 10-day-old wild-type (*WT*; *Col*) and *rtd1-1* seedlings. *B*, base of the main stem in WT and *rtd1-1* plants show a reduced number of trichomes in *rtd1-1*. *C*, roots of 4-day-old WT and *rtd1-1* seedlings show an increased number of root hair cells in *rtd1-1*. *Bar* = 5 mm in *B* and 1 mm in *C*.

dried seedlings were mounted on scanning electron microscopy stubs with double-sided mounting tape, then coated with gold and examined by scanning electron microscopy (Hitachi S-2460, Tokyo, Japan).

Protoplast Transient Expression and Bimolecular Fluorescence Complement (BiFC) Assays—To generate the necessary constructs, the full-length coding sequences of the genes were inserted into *pUC-SPYNE* or *pUC-SPYCE* (51) using XbaI and BamHI. The plasmids were extracted and purified using a Plasmid Maxprep kit (Vigorous) according to the manufacturer's protocol. Protoplasts were produced from 3–4-week-old *Arabidopsis* leaves grown under short-day conditions (8 h of light/16 h of dark) and transformed with purified plasmid using polyethylene glycol (52). After 12–18 h of incubation at 22 °C in the dark, the transformed protoplasts were checked for YFP fluorescence by confocal laser scanning microscopy (LSM 510 META; Zeiss). To confirm that AtMYC1 was expressed normally, protoplasts transformed with the corresponding plasmids were collected, and their proteins were probed with anti-c-Myc antibodies by Western blotting.

Yeast Two-hybrid Interaction Assay—To generate the plasmids for this assay, the coding sequences of the tested genes were cloned into *pGADT7* and *pGBKT7*. After confirmation by sequencing, the plasmids were transformed into yeast strain AH109. Yeast transformation, growth on S.D. medium, yeast protein extraction by the urea/SDS method, and quantitative β-galactosidase assays were carried out according to the Clontech Yeast Protocols Handbook.

RESULTS

Isolation of Arabidopsis Mutant rtd1-1 (reduced trichomes density)—As trichomes are an easily accessible model for investigating cell fate determination (1, 3, 4), we focused on mutants with trichome developmental defects. In a screen of a T-DNA insertion library, a mutant named *rtd1-1* with fewer rosette leaf trichomes than in wild type was identified (Fig. 1*A*; Table 1). The defect in trichome number remained obvious when the plants bolted; few trichomes were found at the base of the main stem (Fig. 1*B*). Besides the trichome defect, *rtd1-1* had a moderate increase of root hairs (about 16.4% more than the wild type), due to the change of about 30.3% non-hair to hair cells (Fig. 1*C*; Table 2). The flanking sequence of *rtd1-1* was obtained by TAIL-PCR; however, it did not link to the mutant phenotype. So it suggested that there must be another mutation.

TABLE 1
Trichome number of the first and second pair of leaves of wild-type, *Atmyc1*, and transgenic complemented plants

Genotype	Number of trichomes per leaf	
	First leaf pair[a]	Second leaf pair[a]
WT	27.15 ± 3.25	39.29 ± 3.96
Atmyc1-1 (rtd1-1)	10.12 ± 1.56	14.92 ± 2.83
Atmyc1-2	10.31 ± 2.15	15.15 ± 3.02
Atmyc1-3	13.85 ± 2.53	14.81 ± 2.62
Re-1-1	30.88 ± 6.85	39.27 ± 9.28
Re-2-14	31.81 ± 6.00	42.48 ± 8.83

[a] The values presented are the average ± S.D. For each line 12 plants were examined.

Phenotypes of rtd1-1 Are Attributed to Point Mutation in bHLH Gene AtMYC1—To determine the genetic background of *rtd1-1*, the mutant (Col background) was crossed with wild-type Col plants. Among 96 B3 lines (*i.e.* third backcross generation), 28 lines (15 plants were tested per line) showed reduced trichome density defect. Therefore, we concluded that the defect was caused by a recessive mutation.

To identify the mutated gene responsible for these defects, the *rtd1-1* was crossed with wild-type L*er* plants for positional cloning. Fine mapping with 183 plants pinpointed the mutation to a 26-kb region between BAC clones *F5I10* and *F6N23* on chromosome 4. Sequencing revealed a point mutation (G518A) in the open reading frame of *AtMYC1* (At4g00480), resulting in an R173H substitution in the protein (Fig. 2*A*). We, therefore, renamed the mutant *Atmyc1-1*.

A homogeneous alignment showed that *AtMYC1* belongs to the bHLH transcription factor IIIf superfamily, which includes *GL3*, *EGL3*, and *TT8* (37). *AtMYC1* encodes a protein of 526 amino acids. The percent identity between AtMYC1 and EGL3, GL3, and TT8 was ~34.3, 34.0, and 30.1%, respectively. Residue Arg-173 in AtMYC1 was conserved among its homologs (Fig. 2*B*).

To confirm that the phenotypes we observed were caused by the mutation in *AtMYC1*, two additional T-DNA alleles of *AtMYC1*, *Atmyc1-2* and *-3*, were characterized. The T-DNA insertion in *Atmyc1-2* was in exon 3; no full-length transcript was detected in homozygous plants. The insertion in *Atmyc1-3* was in the 3′-UTR; semiquantitative and quantitative real-time PCR showed that it was a knock-down allele (Fig. 3, *A* and *B*).

TABLE 2

Effect of *AtMCY1*, *GL3*, and *EGL3* mutation on cell type pattern in the root epidermis

Data, including S.D., were obtained from at least 20 four-day-old seedling roots from each strain. In all strains ~40% of epidermal cells in the Hair cell position.

Genotype	Hair cells in epidermis	Hair cell position		Non-hair cell position	
		Hair cells	Non-hair cells	Hair cells	Non-hair cells
	%	%	%	%	%
WT (Col)	41.8 ± 2.0	98.5 ± 0.7	1.0 ± 0	4.0 ± 2.8	96.0 ± 2.8
Atmyc1-1 (rtd1-1)	58.2 ± 3.7	98.6 ± 0.6	1.5 ± 0.6	30.3 ± 5.0	69.8 ± 5.0
Atmyc1-2	52.4 ± 3.4	99.0 ± 0	1.0 ± 0	20.1 ± 3.8	79.9 ± 3.8
Atmyc1-3	55.8 ± 2.0	98.6 ± 0.8	1.4 ± 0.8	24.7 ± 7.6	75.3 ± 7.6
Re-1-1	40.6 ± 2.0	97.0 ± 1.5	3.0 ± 1.5	2.0 ± 1.0	98.0 ± 1.0
Re-2-14	43.0 ± 3.1	97.6 ± 0.8	2.4 ± 0.8	3.5 ± 0.2	96.5 ± 0.2
gl3-11	70.8 ± 4.5	98.1 ± 1.4	1.9 ± 1.4	50.3 ± 5.7	49.7 ± 5.7
egl3-7	47.0 ± 2.5	98.5 ± 0.8	1.5 ± 0.8	9.6 ± 0.5	90.4 ± 0.5
Atmyc1-1 gl3-11	99.6 ± 0.6	100 ± 0	0 ± 0	99.3 ± 0.9	0.7 ± 0.9
Atmyc1-1 egl3-7	71.0 ± 2.0	99.0 ± 0	1.0 ± 0	51.5 ± 4.5	48.5 ± 4.5
gl3-11 egl3-7	99.0 ± 1.4	100 ± 0	0 ± 0	98.3 ± 2.4	1.7 ± 2.3
Atmyc1-1 gl3-11 egl3-7	100 ± 0	100 ± 0	0 ± 0	100 ± 0	0 ± 0

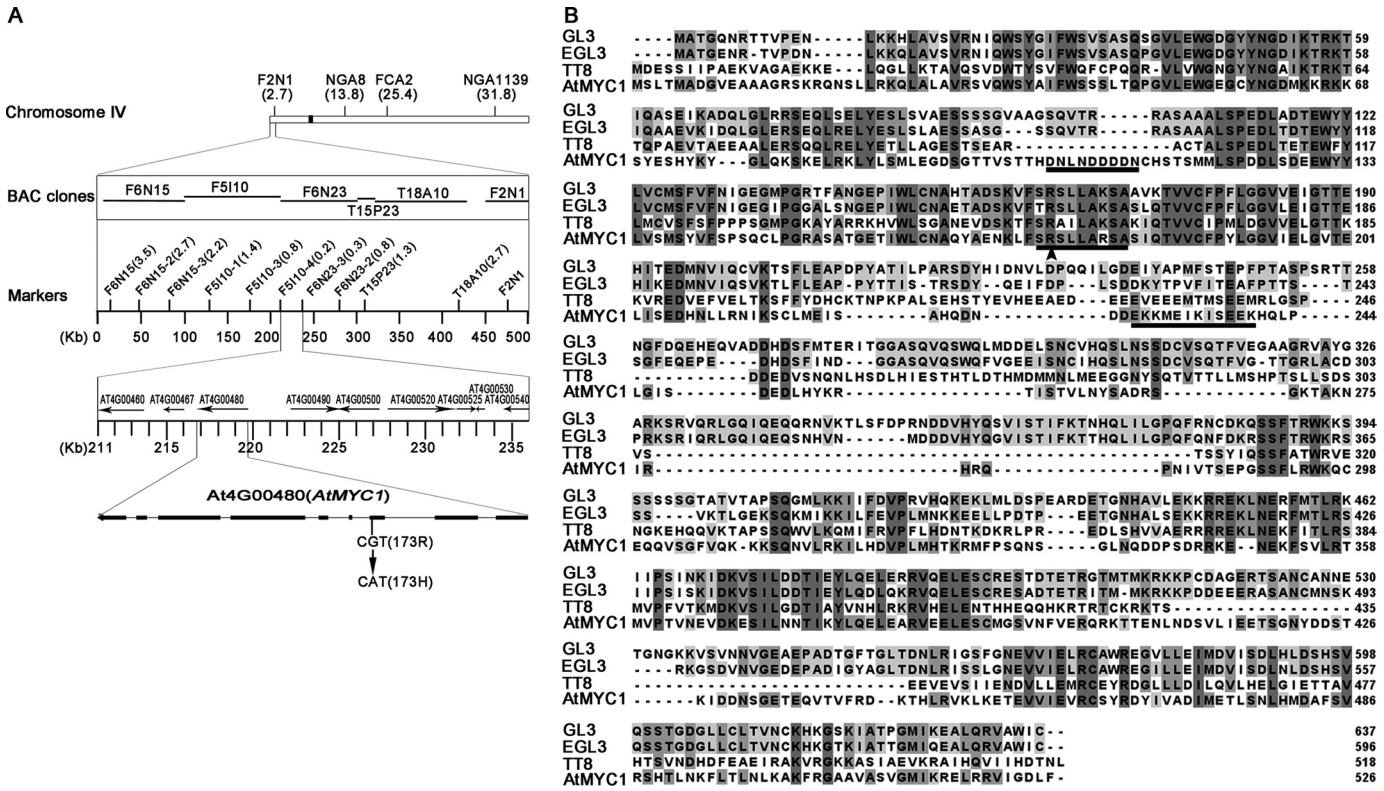

FIGURE 2. **The defects in the mutant were caused by a point mutation in *AtMYC1*.** *A*, shown is positional cloning of *Atmyc1-1*. The *numbers beside the markers* indicate the rates of recombination (%). *B*, alignment of AtMYC1 with bHLH IIIf subfamily homologs from *Arabidopsis* is shown. Identical amino acids are shown in *black*; conserved residues are shown in *gray*. The *black arrowhead* shows the position of the mutation in *Atmyc1-1*. The *underlined motifs* are LCRs in AtMYC1 predicted by SMART.

Both alleles showed similar defects to *Atmyc1-1*, including decreased trichomes (Fig. 3, *C* and *D*; Table 1) and increased root hairs (Fig. 3*E*; Table 2). Furthermore, all these defects were successfully rescued by introducing the wild-type *AtMYC1* coding sequence driven by its native promoter into *Atmyc1-1*. Among 54 independent lines, 36 had similar numbers of trichomes as wild type. Re-1-1 and -2-14 are two representative recovered lines (Fig. 3, *C–E*; Tables 1 and 2). Therefore, we concluded that the defects in the mutants were caused by a loss of function of *AtMYC1*.

AtMYC1 Is Required for Full GL2 Expression—We next focused on the epidermal cell determination defects in *Atmyc1* mutants. To further explore the role of *AtMYC1* in trichome and root hair determination, we examined the expression level of *GL2* in *Atmyc1*, *GL2* is a crucial transcription factor in trichome and non-hair cell development (16–20), and it has been shown to be a direct target of the GL1-GL3-TTG1 complex (13, 53). We, therefore, examined the expression level of *GL2* in *Atmyc1* by quantitative real-time PCR. As expected, *GL2* was down-regulated in all three alleles of *Atmyc1* (Fig. 4*A*) in accordance with the reduction in trichomes and increase in root hairs in *Atmyc1* (Fig. 3*C*-E; Tables 1 and 2). This finding demonstrates that the lesion in *AtMYC1* causes the incomplete *GL2* expression and *AtMYC1* is a positive regulator of GL2.

Genetic Interaction between AtMYC1 and GL3/EGL3—To assess the genetic relationship between *AtMYC1* and its homolog *GL3/EGL3*, *Atmyc1-1* was crossed with the T-DNA insertion mutant *gl3-11* and *egl3-7* (Col background) (54). *gl3-11*

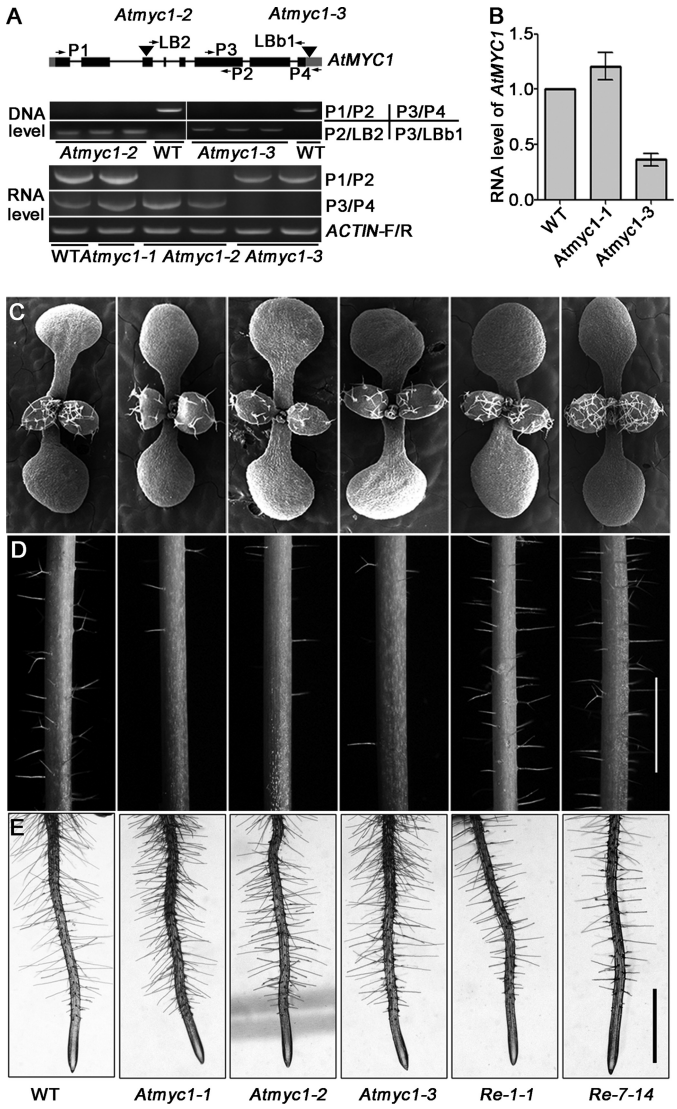

FIGURE 3. **Characterization of T-DNA insertion mutants of *AtMYC1* and a transgenic complementation assay.** *A*, shown are insertion sites in the two T-DNA insertion alleles and characterization of the DNA and RNA levels. *B*, shown is *AtMYC1* expression analysis by quantitative real-time PCR using RNA from 10-day-old plants. *AtMYC1* expression was normalized to that in wild type; *ACTIN* was used as an endogenous control. Three biological replicates were performed. *Error bars* indicate the S.D. from the three biological replicates. shown are scanning electron micrographs of 10-day-old plants (*C*), base of the main stem (*D*), and roots of 4-day-old seedlings (*E*) of the indicated genotypes. Re-1-1 and -7-14 are two independent T3 complementation lines of *pAtMYC1*::*AtMYC1*. *Scale bar* = 2.5 mm in *D* and 1 mm in *E*.

exhibited a moderate decrease in trichome number and an increase in hair cell production, whereas the *egl3-7* largely behaved like the wild type (Fig. 4, *B* and *C*; Table 2).

The *gl3 egl3* double mutant produces both glabrous aerial organs and extremely hairy underground organs (14, 54, Fig. 4, *B–D*; Table 2), which suggested the significant functional redundancy between *GL3* and *EGL3*. For the leaf trichome development, although the *Atmyc1-1 gl3-11* and *Atmyc1-1 egl3-7* double mutants showed a reduction in the trichomes number on the first and second pair of leaves than *Atmyc1-1* (*t* test: $p = 0.048$ and 0.001, respectively; Fig. 4, *B* and *C*), the degree of reduction was much less than that of the *gl3 egl3* double mutant. However, *Atmyc1-1 gl3-11* show glabrous inflorescence stem (Fig. 4*D*) and hairy root defects with 99.6% hair cells in root epidermis because of the misspecification of non-hair to hair cells (Table 2). These results suggest that *AtMYC1* and *GL3* function redundantly in stem trichome and root hair cell fate control and only partially redundant in leaf trichome control.

Furthermore, we analyzed the *Atmyc1-1 egl3-7* double mutant, which had a slight decrease of leaf trichome (Fig. 4, *B* and *C*), moderate increase of root hair number (Table 2), and almost no change of stem trichomes compared with the parental line *Atmyc1-1* (Fig. 4*D*). These results indicate that the degree of redundancy between *AtMYC1* and *EGL3* is even less than that of *AtMYC1* and *GL3*.

To further analyze the functional similarity and divergence of *AtMYC1* and its homologs, we designed a promoter exchange assay. A 2.5- and 3-kb intergenic region upstream of ATG of *GL3* and *EGL3*, respectively, were fused before the coding region of *AtMYC1*, and a 2.58-kb intergenic region upstream of start codon of *AtMYC1* was fused ahead the open reading region of *GL3* or *EGL3*. The constructs *pAtMYC1*::*GL3* and *pAtMYC1*::*EGL3* were introduced to *Atmyc1-2*, whereas *pGL3*::*AtMYC1* and *pEGL3*::*AtMYC1* were transformed into *gl3-11 egl3-7* double mutant. We observed that both *GL3* and *EGL3* driven by *AtMYC1* promoter successfully rescued the reduced trichomes defect of *Atmyc1-2* (Fig. 4*E*, *lower panel*); however, *AtMYC1* driven by *pGL3* and *pEGL3* were not able to complement the *gl3 egl3* double mutant phenotype at all (Fig. 4*E*, *lower panel*). As controls, *pAtMYC1*::*AtMYC1*, *pGL3*::*GL3*, and *pEGL3*::*EGL3* were able to recover the corresponding mutant trichome defects (Fig. 4*E*, *top panel*), and the *pGL3/EGL3*::*AtMYC1* constructs were functional because they can rescue the *Atmyc1-2* phenotype (Fig. 4*E*, *lower panel*). Similar results were obtained for the root hair cell fate determination (Table 3). These results indicate that GL3/EGL3 can exert the activity of AtMYC1 in leaf trichome specification, whereas AtMYC1 cannot substitute either GL3 or EGL3 in leaf trichome and root hair development *in planta*. These results together demonstrate that the function of AtMYC1 and GL3/EGL3 is both similar/redundant and divergent.

Expression Pattern of AtMYC1—To better define the expression pattern of *AtMYC1* during root hair and trichome development, we created *pAtMYC1*::*GUS* construct and transformed it into the wild-type. We analyzed the transgenic plants for GUS expression pattern. Consistent with the defects in root hair spacing seen in *Atmyc1*, *AtMYC1* was expressed in alternate cell files in the roots (Fig. 5*A*). Enlarged views of the meristematic and root hair zones revealed that the deeply stained cells were hair cell files. Because the stained cells files in the meristematic zone were located in a cleft between two underlying cortical cells and had a higher division rate than the neighboring unstained ones, they were in the same cell files with GUS-staining cells, producing root hairs in the mature region (Fig. 5, *B* and *C*). This expression pattern of *AtMYC1* is similar to that of its homologs *GL3* and *EGL3* (55). In the rosette leaf, *pAtMYC1*::*GUS* expression was detected in the basal cells of trichomes (Fig. 5, *D* and *E*), in contrast to its homologs, which had higher expression in trichomes (13). Finally, we detected

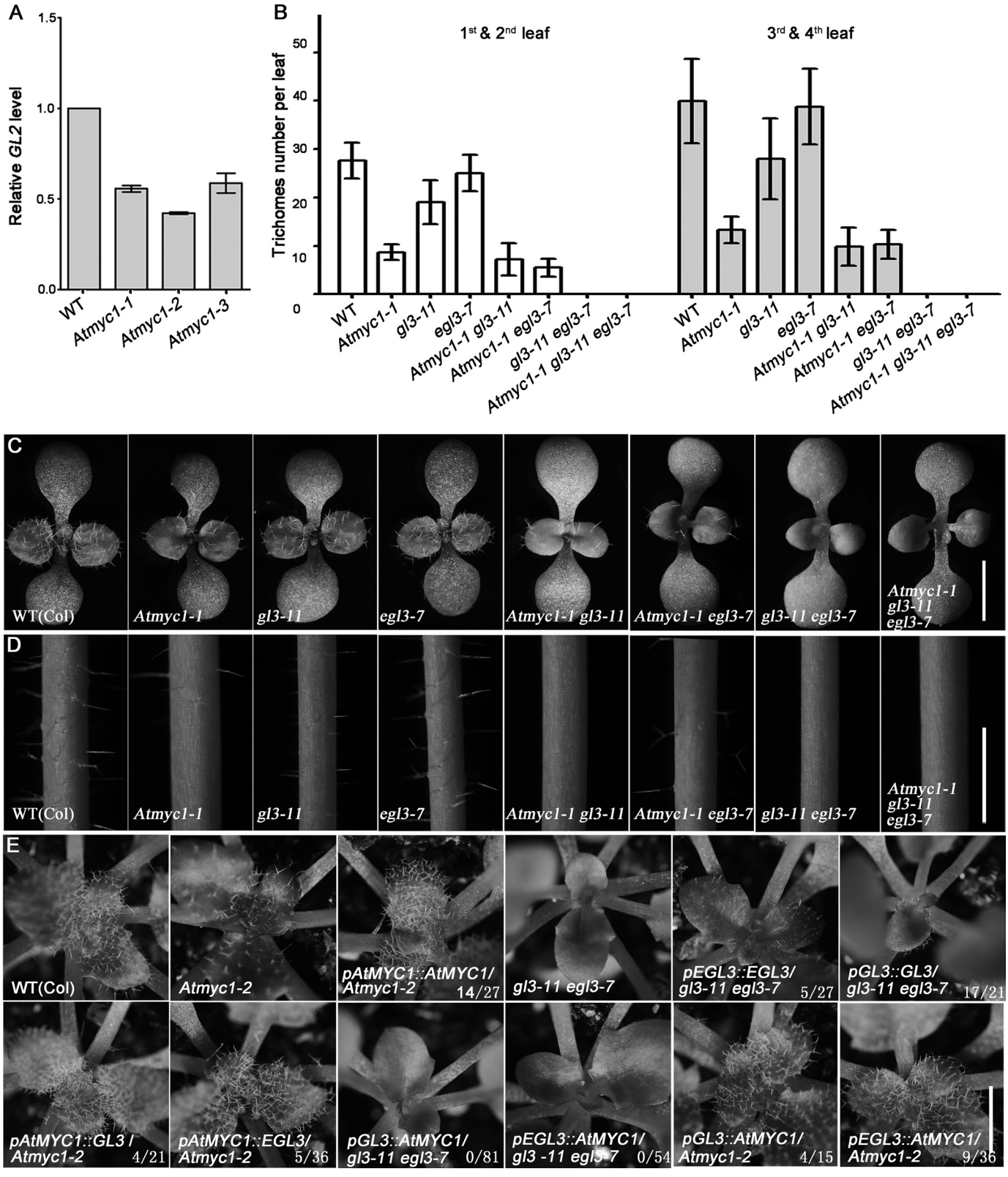

FIGURE 4. **Functional relationship between *AtMYC1* and *GL3/EGL3*.** *A*, shown is *GL2* expression in 10-day-old plants as detected by quantitative real-time PCR. The expression levels of *GL2* in *Atmyc1* were normalized to that in wild type. *ACTIN* was used as an endogenous control. Three biological replicates were performed. *Error bars* indicate the S.D. from the three biological replicates. *B*, trichome number analysis in the first to fourth pair of leaves in single, double, and triple mutants of *Atmyc1-1 gl3-11* and *egl3-7*. At least 12 plants were analyzed for each genotype. *Error bars* represent the S.D. Shown are 10-day-old plants (*C*) ad the base of the inflorescence stem (*D*) of the indicated genotypes, respectively. *E*, shown is the promoter exchange assay to test the similarity or divergence of AtMYC1 and GL3/EGL3. Pictures are of three-week-old plants. *Numbers* at the *bottom of the pictures* show the transgenic complementation lines from the total independent transgenic lines examined. *Scale bar* = 2 mm in *C*, *D* and *E*.

TABLE 3

Effect of promoter exchange on cell type pattern in the root epidermis

Data, including S.D. were obtained from at least 20 four-day-old seedlings from each strain. In all strains, ~40% of epidermal cells in the Hair cell position.

Genotype	Hair cells in epidermis	Hair cell position		Non-hair cell position	
		Hair cells	Non-hair cells	Hair cells	Non-hair cells
	%	%	%	%	%
WT (Col)	41.2 ± 0.6	99.0 ± 0	1.0 ± 0	2.7 ± 0.9	97.3 ± 0.9
Atmyc1-2	50.2 ± 0.3	99.0 ± 0	1.0 ± 0	17.7 ± 0.5	82.3 ± 0.5
gl3-11 egl3-7	100 ± 0	100 ± 0	0 ± 0	100 ± 0	0 ± 0
pGL3::GL3/gl3 egl3	47.6 ± 5.1	95.0 ± 0	5.0 ± 0	16.0 ± 8.5	84.0 ± 8.5
pEGL3::EGL3/gl3 egl3	52.3 ± 0.1	99.0 ± 0	1.0 ± 0	20.3 ± 2.4	79.7 ± 2.4
pAtMYC1::GL3/Atmyc1-2	40.6 ± 1.4	95.2 ± 1.3	4.8 ± 1.3	1.0 ± 1.5	99.0 ± 1.5
pAtMYC1::EGL3/Atmyc1-2	42.6 ± 2.5	98.1 ± 1.4	1.9 ± 1.4	0.7 ± 1.0	99.3 ± 1.0
pGL3::AtMYC1/gl3 elg3	95.6 ± 6.2	100 ± 0	0 ± 0	92.7 ± 10.4	7.3 ± 10.4
pEGL3::AtMYC1/gl3 elg3	99.8 ± 0.3	100 ± 0	0 ± 0	99.7 ± 0.5	0.3 ± 0.5

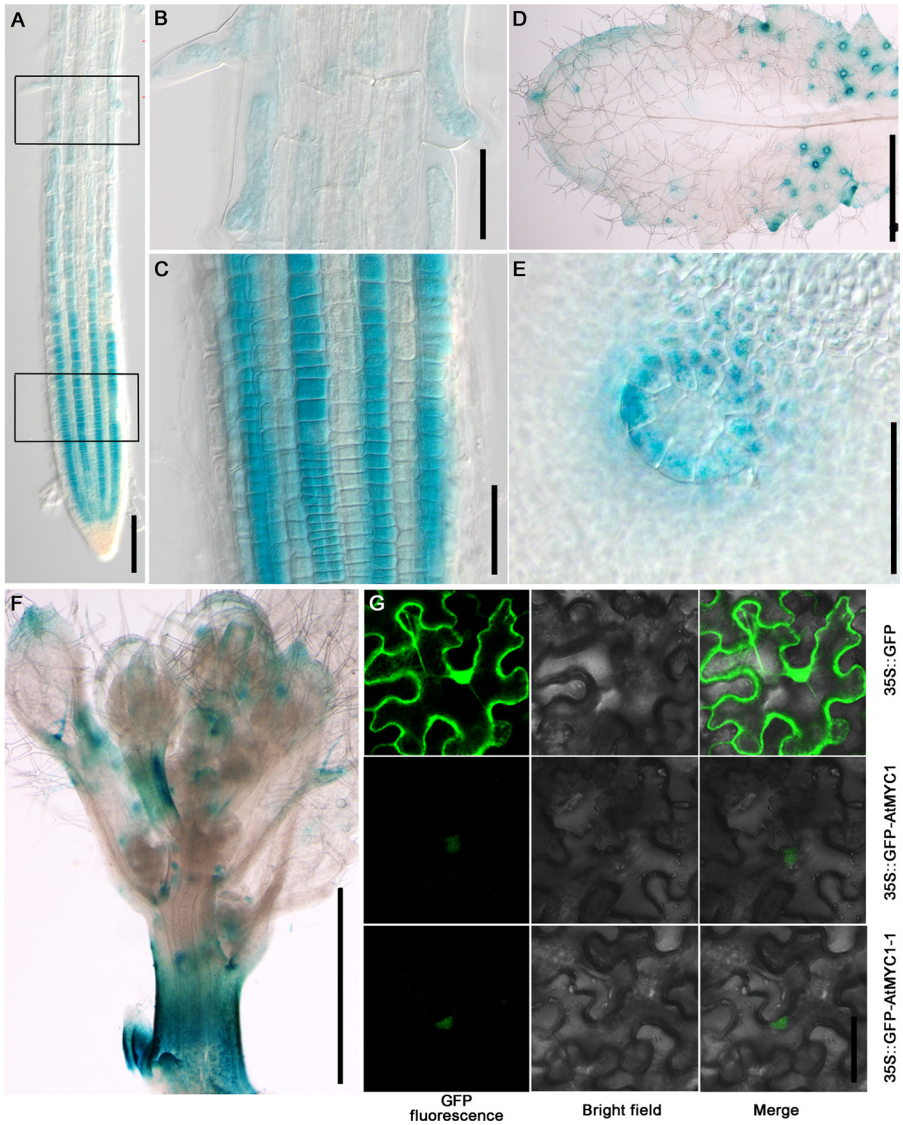

FIGURE 5. **AtMYC1 expression pattern.** *A*, shown is an overall view of *pAtMYC1::GUS* in root hair cell files. *B* and *C*, shown are enlarged views of the *boxed region in A*. *D*, shown is expression of *pAtMYC1::GUS* in the rosette leaves. *E*, shown is an enlarged view of *D*. *F*, shown is expression of *AtMYC1* at the base of the main stem. *Scale bar* = 100 μm in *A*, 50 μm in *B*, *C*, *E*, and *G*, 2 mm in *D*, and 1 mm in *F*.

strong GUS activity at the base of the inflorescence stem, consistent with the reduced number of trichomes in this region (Fig. 5*F*). In conclusion, the pattern of *AtMYC1* expression shown using *GUS* is largely consistent with its biological functions.

AtMYC1 Functions through Its Interaction with MYB Proteins and TTG1—It was previously reported that the bHLH proteins GL3 and EGL3 interact with GL1/WER and TTG1 to promote trichome and non-hair cell identity (13–15, 56). And it was reported that AtMYC1 also interacted with these proteins

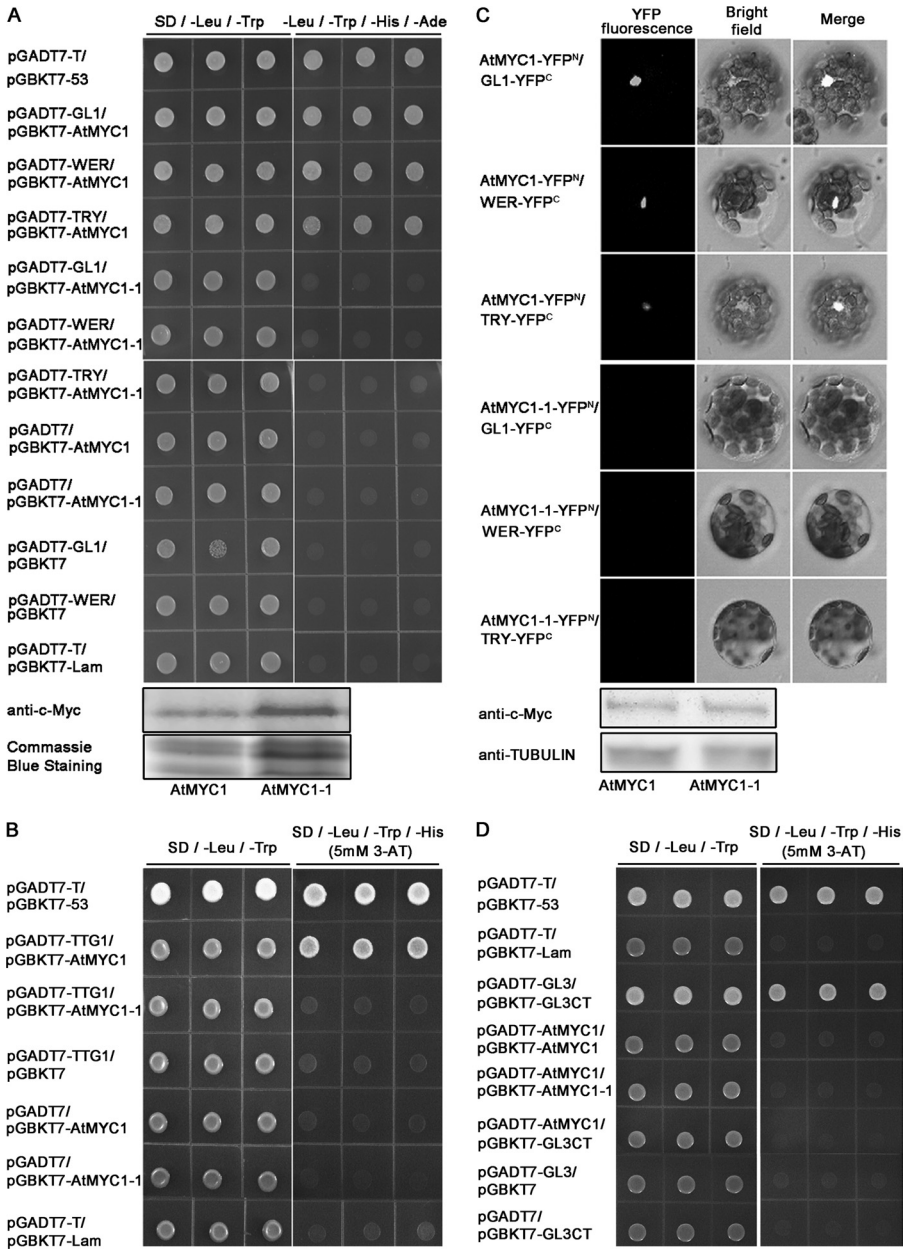

FIGURE 6. **Physical interaction between AtMYC1 and MYB proteins, TTG1.** *A*, physical interaction between AtMYC1 and MYB proteins is shown by a yeast two-hybrid assay. Positive control: pGADT7-T/pGBKT7–53; negative control: pGADT7-T/pGBKT7-Lam. The interaction between AtMYC1/AtMYC1-1 and MYB proteins was assessed by growth on SD/−Ade/−His/−Leu/−Trp medium. Wild-type and mutated AtMYC1 were expressed in yeast and examined by Western blotting. *B*, physical interaction between AtMYC1/ AtMYC1-1 and TTG1 in yeast is shown. *C*, a BiFC assay to test the interaction between AtMYC1/ AtMYC1-1 and MYB proteins is shown. AtMYC1 and AtMYC1-1 expression in *Arabidopsis* protoplasts was examined by Western blotting. *D*, shown is yeast two-hybrid analysis of AtMYC1 dimerization. *B* and *D*, protein-protein interactions were assessed by growth on SD/−Leu/−Trp/−His medium containing 5 mM 3-AT.

in vitro (45). We confirmed the interaction in a yeast two-hybrid assay (Fig. 6, *A* and *B*). We next conducted an *in vivo* BiFC assay to confirm these results in transiently transfected *Arabidopsis* mesophyll cell protoplasts. For AtMYC1-YFP^N/GL1-YFP^C, AtMYC1-YFP^N/WER-YFP^C, and AtMYC1-YFP^N/TRY-YFP^C, about 5, 16, and 5% of the protoplasts produced strong YFP fluorescence (Fig. 6*C*); in comparison, no interaction signal was observed in the negative controls (AtMYC1-1-YFP^N/Target protein-YFP^C). Therefore, we concluded that AtMYC1 interacts with the MYB proteins and TTG1.

Because GL3 and EGL3 have the ability to form homo- and heterodimers in yeast (14, 15), we analyzed the dimerization of AtMYC1. GL3 dimerization was detected; however, AtMYC1 formed neither homo- nor heterodimers (Fig. 6*D*). Thus, similar to its homologs, AtMYC1 may be involved in an interaction with MYB proteins and TTG1; however, it does not dimerize. The inability of AtMYC1 to form dimer may be the reason for its failure to rescue *gl3 egl3* double mutant.

Arg-173 in AtMYC1 Is Critical for Its Interaction with MYB Proteins and TTG1—Because the only mutation in *Atmyc1-1* was R173H, we sought to determine the reason for its failure in function. We proposed several hypotheses; the mutation might alter the stability of *AtMYC1* mRNA, the subcellular localization of AtMYC1-1 might be altered, or its ability to interact with

its binding partners might be affected. To test these hypotheses, we first assessed the level of expression of *AtMYC1* in *Atmyc1-1* by semiquantitative and quantitative PCR. We found that the expression level of *AtMYC1* was unaffected (Fig. 3, *A* and *B*). The subcellular localization of the wild-type and mutated forms of AtMYC1 was also analyzed. Both the wild-type and mutant proteins could localize to the nucleus in tobacco leaf cells after *Agrobacterium* infiltration (Fig. 5*G*). Thus, the subcellular localization of AtMYC1-1 was not altered by the mutation either.

Next, protein-protein interactions were examined. As described above, AtMYC1 interacted with GL1, WER, TRY, and TTG1 (Fig. 6. *A–C*). Thus, we examined the interaction between AtMYC1-1 and MYB proteins, TTG1. Wild-type AtMYC1 was able to interact with GL1, WER, TRY, and TTG1 as shown by its growth on SD/−Ade/−His/−Leu/−Trp medium (Fig. 6, *A* and *B*). However, this was not true for AtMYC1-1 carrying the R173H substitution. This mutation resulted in an inability to grow on SD/−Ade/−His/−Leu/−Trp medium (Fig. 6*B*), indicating abolishment of the interaction between AtMYC1 and MYB proteins, TTG1. This result was confirmed *in vivo* by a BiFC assay in transiently transfected *Arabidopsis* mesophyll cell protoplasts. Protoplasts cotransfected with AtMYC1-YFP^N/GL1-YFP^C, AtMYC1-YFP^N/WER-YFP^C, and AtMYC1-YFP^N/TRY-YFP^C exhibited strong YFP fluorescence (Fig. 6*C*). In terms of AtMYC1-1-YFP^N/GL1-YFP^C, AtMYC1-1-YFP^N/WER-YFP^C, and AtMYC1-1- YFP^N/TRY-YFP^C, no YFP signal was produced using the first two pairs, whereas about 2% of the AtMYC1-1-YFP^N/TRY -YFP^C cells showed YFP fluorescence (reduced by 60% relative to its wild-type counterpart) (Fig. 6*C*). These results indicated that the inability of AtMYC1-1 to interact with MYB proteins and TTG1 may account for its loss of function and the trichome and root hair patterning defects we observed. These results further suggest that the Arg-173 residue in AtMYC1 is required for its interaction with its binding partners and for its biological function.

Low Complexity Regions (LCRs) and Interaction of AtMYC1 with Its Partners—To explore the possibility that the R173H mutation affected the domain architecture of AtMYC1, we analyzed the mutated protein using the SMART and NCBI protein domain prediction websites. There are three LCRs in wild-type AtMYC1 besides the bHLH domain, and the R173H mutation abolished the second one (Fig. 7*A*). Because proteins with LCRs tend to have more partners than those without, indicating a role for LCRs in protein-protein interactions (57), we examined the influence of the LCRs in AtMYC1 on its ability to interact with MYB proteins. Several point mutations were introduced into the LCRs to enable us to test their role in protein-protein interactions by yeast two-hybrid analysis. Among the mutations introduced were: R178H, which was located in the same LCR as R173; S174A, another residue in the same LCR; N106A and I234A in the first and third LCRs, respectively (Fig. 7*A*). AD-GL1 and the different BD-AtMYC1s were cotransformed into yeast and analyzed for β-galactosidase activity. Only the R178H mutation resulted in partial reduction of enzyme activity. The other three mutations did not affect the amount of

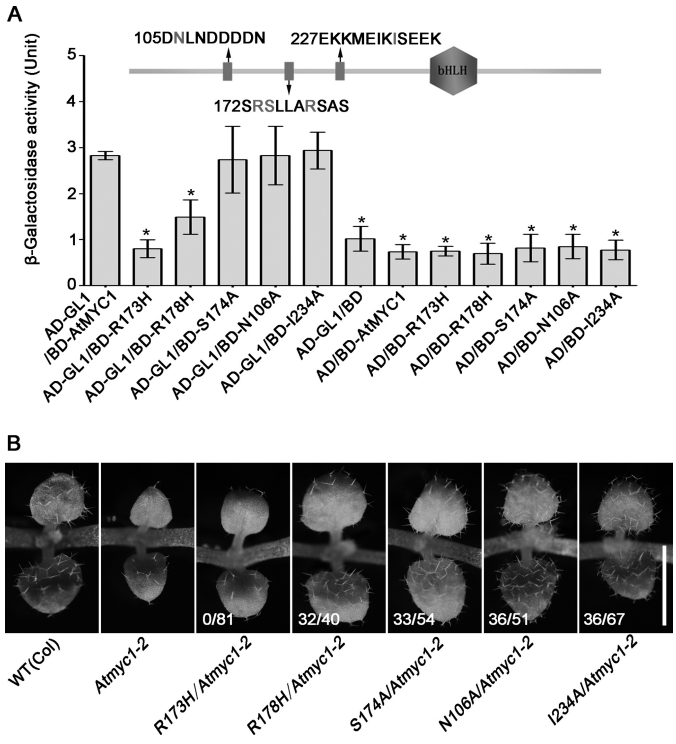

FIGURE 7. **The functional analysis of LCRs in AtMYC1.** *A*, analysis of the effect of LCRs on the interaction of AtMYC1 with its binding partners by measuring β-galactosidase activity in yeast is shown. Three biological replicates were performed for each experiment. *Error bars* indicate the S.D. from the three biological replicates. *Asterisks* denoted significantly different from the wild-type AtMYC1/GL1 control ($p < 0.05$, Student's *t* test). The diagram shows the structure of AtMYC1 as revealed by SMART. The three LCRs are indicated by *boxes*; the amino acids in each LCR are shown nearby. The *letters in gray* are the residues that were mutated to abolish the LCR motifs; *numbers* indicate the locus of the first amino acid residue in each LCR in AtMYC1. *B*, shown is functional analysis of LCR mutations *in planta*. Native promoter was used to promote different point mutations. These constructs were transformed into *Atmyc1-2* background. Pictures were taken for the trichomes on the first pair of true leaves from 12-day-old plants. *Numbers in the bottom of picture* show the transgenic complementation lines from the total independent transgenic lines examined. *Scale bar* = 2 mm in *B*.

β-galactosidase activity despite the fact that they abolished the LCRs (Fig. 7*A*).

To further test the effect of these mutations, the mutant form of AtMYC1s were driven by its native promoter and transformed into *Atmyc1-2*. AtMYC1-1 could not rescue *Atmyc1-2* phenotype among 81 independent T1 lines (Fig. 7*B*), indicating full abolishment of the AtMYC1 function by the R173H mutation. However, the other four mutant forms of AtMYC1s could successfully recover mutant phenotype (Fig. 7*B*), demonstrating that these mutations did not obviously affect protein activity *in vivo*. Thus, the Arg-173 residue in AtMYC1, other than the LCRs, is crucial for the interaction of AtMYC1 with MYB proteins.

Conserved Arg Residue Is Also Essential for Interaction of AtMYC1 Homologs with Their Partners—Because our alignment showed that residue Arg-173 was conserved among AtMYC1 and its closest homologs (GL3, EGL3, and TT8) (Fig. 2*B*), we predicted that the corresponding Arg in AtMYC1 homologs may contribute to their protein-protein interactions. To test this, we examined the effect of the conserved Arg mutation on EGL3 and GL3 protein-protein interactions. As before,

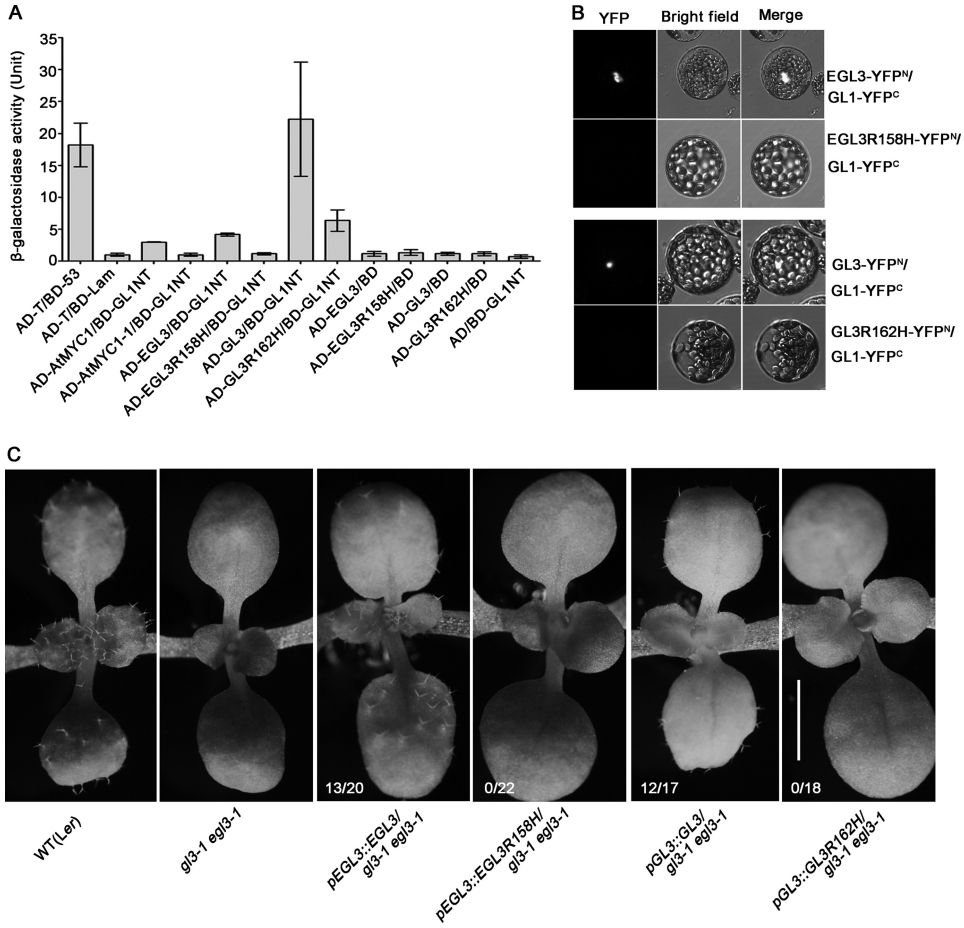

FIGURE 8. **The conserved Arg residue in AtMYC1 is functionally conserved among the IIIf subfamily of bHLH transcription factors.** *A*, shown is analysis of the importance of the conserved Arg in EGL3/GL3 for their interaction with other proteins based on the level of β-galactosidase activity in yeast. *Error bars* indicate the S.D. from three biological replicates. *B*, a BiFC assay tests the effect of mutation of EGL3R158H and GL3R162H on interaction with GL1, respectively. *C*, a transgenic complementary assay tests the mutation of conserved Arg in EGL3 and GL3 on their protein function *in planta*. Trichomes on the first and second pair of true leaves from 2-week-old plants were taken pictures. *Numbers in the bottom of picture* show the transgenic complementation lines from the total independent transgenic lines examined. *Scale bar* = 2 mm in *C*.

the Arg residue was changed to a His and inserted into yeast two-hybrid vectors. Like full-length GL1, GL3 has strong self-activation when fused to the DNA-binding domain of GAL4. Because the N terminus of GL1 (GL1NT), which contains the MYB repeat domain, has been shown to successfully interact with GL3/EGL3 without autoactivation (15), we constructed BD-GL1NT and AD-GL3/EGL3 and tested their interactions by yeast two-hybrid analysis and the measurement of β-galactosidase activity. The Arg-to-His mutation in EGL3 affected its interaction with GL1; reduced β-galactosidase activity relative to that in the negative control was observed (Fig. 8*A*). In the case of GL3, β-galactosidase activity was decreased by about 70% (Fig. 8*A*). In our BiFC assays, about 10 and 0.01% of the co-transformed protoplasts exhibited strong YFP fluorescence in their nuclei for wild-type EGL3-YFP^N/GL1-YFP^C and EGL3R158H-YFP^N/GL1-YFP^C, respectively, indicating that the Arg residue substitution abolished the EGL3/GL1 interaction *in vivo* (Fig. 8*B*). Similar results were obtained for GL3 and GL3R162H; the percentage of cells exhibiting fluorescence was 19 and 5%, respectively, when co-transfected with GL1 (Fig. 8*B*).

We further tested the importance of this conserved Arg *in planta* by introducing the point mutation form of protein into *gl3 egl3* double mutant. Consistently, among 18 independent T1 lines, no trichome was produced in *pEGL3*::*EGL3R158H* transgenic plants (Fig. 8*C*). As a control, the *pEGL3*::*EGL3* recovered trichome production in 12 independent lines among 17 (Fig. 8*C*). Similarly, *pGL3*::*GL3R162H* failed to complement the glabrous defect of *gl3 egl3* double mutant among 22 independent lines, whereas the *pGL3*::*GL3* induce trichome production in 13 independent lines among 20 (Fig. 8*C*). TT8 was not examined here, as it mainly functions in seed pigment synthesis and does not interact with GL1 (58). Taken together, we identified a conserved Arg residue IIIf bHLH family member that is essential for the proper function and interaction of R/B-like IIIf bHLH proteins with their binding partners.

DISCUSSION

AtMYC1 Controls Trichome and Root Hair Cell Fate Determination in Arabidopsis—We isolated an *AtMYC1* mutant with defects in trichome and root hair pattern formation (Fig. 1; Tables 1 and 2). The characterization of two additional T-DNA insertion alleles and the transgenic complementation assay confirmed that *AtMYC1* is involved in trichome and root hair patterning in *Arabidopsis* (Fig. 3).

Our results show that *AtMYC1* functions in trichome and root hair control together with MYB proteins and TTG1 (Fig. 6). *GL2*, the immediate downstream target of MYB-GL3-TTG1, was down-regulated in all alleles of *Atmyc1* (Fig. 4*A*), consistent with the observed phenotypes of *Atmyc1* (Fig. 3, *C–E*; Tables 1 and 2). We speculate that *GL2* is also a downstream target of *AtMYC1*.

Genetic analysis shows that *AtMYC1* has both function redundancy and divergence with *GL3/EGL3* (Fig. 4). They are involved in trichome and root hair cell fate control redundantly with different degree. The redundancy between *AtMYC1* and *GL3* is obvious for root hair cell and stem trichome development while less obvious for the leaf trichome (Fig. 4, *B–D*; Table 2). The redundancy between *AtMYC1* and *EGL3* is weakest, whereas the strongest is between *GL3* and *EGL3* (Fig. 4, *B–D*; Table 2). Their functional divergences are as follows. First, the phenotypes of *Atmyc1* and *gl3* were different in branch development. *gl3* produced fewer branches (15), whereas *Atmyc1* showed no change in branch number (data not shown). Second, GL3 and EGL3 formed homo- and heterodimers with each other (14, 15); however, AtMYC1 was unable to dimerize under our conditions (Fig. 6*D*). Third, GL3 and EGL3 are capable to complement leaf trichome and root hair phenotype of *Atmyc1*, whereas GL3 and EGL3 are irreplaceable by AtMYC1 for leaf trichome and root hair development (Fig. 4*E*). Fourth, *GL3* overexpression partially rescued the glabrous phenotype of *ttg1*, whereas AtMYC1 overexpression did not (15). In addition, Morohashi and Grotewold (20) found that GL3/GL1 bind to *AtMYC1* chromatin, suggesting that *AtMYC1* functions downstream of *GL3/GL1* and indicating the existence of feed-forward regulation in the function of *AtMYC1* and *GL3*. In conclusion, the functions of *AtMYC1* and *GL3/EGL3* are not simple redundancy. They have similar yet distinct functions during *Arabidopsis* epidermis cell fate determination, which is summarized in a simple model in Fig. 9.

Characterization of Atmyc1-1 Reveals Critical Amino Acid Residue for Interaction of AtMYC1 with MYB Proteins and TTG1—Formation of the MYB-bHLH-TTG1 trimeric complex, in which MYB proteins and TTG1 bind a bHLH transcription factor simultaneously, is important for proper development in *Arabidopsis* (*e.g.* trichome and root hair patterning, flavonoid/anthocyanin metabolism, and mucilage biosynthesis) (4, 12–14, 35, 39, 40). The N-terminal-most 100 amino acid residues and ~200–400 amino acid residues in the bHLH protein GL3 are required for its interaction with MYB proteins and TTG1, respectively (14). Our *in vitro* and *in vivo* results (Fig. 6) and previous yeast two-hybrid or pulldown data (28, 45) indicate that AtMYC1, like other bHLH factors, interacts with MYB proteins and TTG1.

We isolated an *AtMYC1* mutant with a defect in trichome and root hair patterning (Fig. 1; Tables 1 and 2). Positional cloning suggested that an R173H mutation in AtMYC1 accounted for the defects in the mutant (Fig. 2*A*). By virtue of a point mutation at Arg-173 in AtMYC1, we verified that this Arg residue is essential for the interaction of AtMYC1 with MYB proteins and TTG1 *in vitro* and *in vivo* (Fig. 6). The failure to interact with its partner proteins in AtMYC1-1 resulted in altered *GL2* expression, leading to defects in trichome and root hair patterning (Figs. 3 and 4*A*; Tables 1 and 2). Thus, this Arg residue is essential for AtMYC1 and MYBs-TTG1 interactions, downstream gene activation, and *Arabidopsis* epidermal cell fate determination.

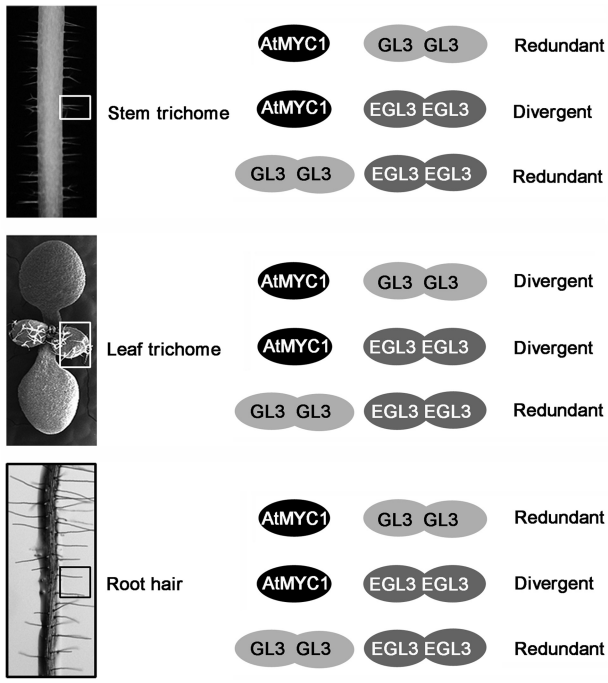

FIGURE 9. **The comparison of AtMYC1 and its homologs in trichome and root hair cell fate determination.** AtMYC1 and its homologs are indicated by ellipsoids of different *gray colors*. AtMYC1 cannot form dimers, whereas GL3 and EGL3 both can dimerize, which is shown by a single ellipsoid (monomer) and two overlapped ellipsoids (dimer), respectively. The functional redundancy and divergence for AtMYC1, GL3, and EGL3 in control of trichome of stem and leaf and root hair specification are indicated on the *right*.

Although Arg to His mutation abolished the formation of a LCR, our results showed that the other four mutations that also led to LCRs abolishment did not affect the gene function *in planta* (Fig. 7*B*). These results highlight the importance of this conserved Arg in protein interaction. It was reported that in a high throughput statistical analysis of amino acid frequencies involved in protein interaction, the arginine is the most frequent residue because of its wider radii of action and more accessible long side chains carrying the charge (59). So the Arg to His mutation may change the favorable amino acid feature for protein interaction or alter the protein structure, resulting in failure of interaction with partners.

Arg Residue Is Functionally Conserved among IIIf Subfamily bHLH Transcription Factors—An alignment of AtMYC1 with homologs of the bHLH IIIf subfamily from *Arabidopsis* showed that the critical Arg-173 residue was conserved among its closest homologs (EGL3, GL3, and TT8; Fig. 2*B*), indicating the functional conservation of this amino acid residue. By yeast two-hybrid and BiFC assays and transgenic complementation analysis we showed that the interaction between EGL3/GL3 and MYB protein GL1 and their biological function were affected by the corresponding Arg-to-His mutation (Fig. 8, *A–C*). Thus, our results demonstrate that the corresponding Arg residue in GL3 (Arg-162) and EGL3 (Arg-158) is important for protein interaction. This residue is not in any of the reported

MYB- or TTG1-interacting regions; thus, we revealed a novel critical and functionally conserved site in IIIf bHLH proteins for the protein-protein interaction and proper function.

Acknowledgments—We thank Drs. Jessica Habashi and Zheng Wang for critical reading of the manuscript, Junfeng Zhao for assistance for the image, the ABRC for the T-DNA insertion lines.

REFERENCES

1. Balkunde, R., Pesch, M., and Hülskamp, M. (2010) Trichome patterning in *Arabidopsis thaliana* from genetic to molecular models. *Curr. Top. Dev. Biol.* **91,** 299–321
2. Tominaga-Wada, R., Ishida, T., and Wada, T. (2011) New insights into the mechanism of development of *Arabidopsis* root hairs and trichomes. *Int. Rev. Cell Mol. Biol.* **286,** 67–106
3. Ishida, T., Kurata, T., Okada, K., and Wada, T. (2008) A genetic regulatory network in the development of trichomes and root hairs. *Annu. Rev. Plant Biol.* **59,** 365–386
4. Pesch, M., and Hülskamp, M. (2009) One, two, three . . . models for trichome patterning in *Arabidopsis*? *Curr. Opin. Plant Biol.* **12,** 587–592
5. Kwak, S. H., Shen, R., and Schiefelbein, J. (2005) Positional signaling mediated by a receptor-like kinase in *Arabidopsis*. *Science* **307,** 1111–1113
6. Kwak, S. H., and Schiefelbein, J. (2007) The role of the SCRAMBLED receptor-like kinase in patterning the *Arabidopsis* root epidermis. *Dev. Biol.* **302,** 118–131
7. Kwak, S. H., and Schiefelbein, J. (2008) A feedback mechanism controlling SCRAMBLED receptor accumulation and cell-type pattern in *Arabidopsis*. *Curr. Biol.* **18,** 1949–1954
8. Kwak, S. H., and Schiefelbein, J. (2008) Cellular pattern formation by SCRAMBLED, a leucine-rich repeat receptor-like kinase in *Arabidopsis*. *Plant Signal. Behav.* **3,** 110–112
9. Dolan, L. (2006) Positional information and mobile transcriptional regulators determine cell pattern in the *Arabidopsis* root epidermis. *J. Exp. Bot.* **57,** 51–54
10. Hülskamp, M., Misa, S., and Jürgens, G. (1994) Genetic dissection of trichome cell development in *Arabidopsis*. *Cell* **76,** 555–566
11. Larkin, J. C., Young, N., Prigge, M., and Marks, M. D. (1996) The control of trichome spacing and number in *Arabidopsis*. *Development* **122,** 997–1005
12. Bernhardt, C., Lee, M. M., Gonzalez, A., Zhang, F., Lloyd, A., and Schiefelbein, J. (2003) The bHLH genes GLABRA3 (GL3) and ENHANCER OF GLABRA3 (EGL3) specify epidermal cell fate in the *Arabidopsis* root. *Development* **130,** 6431–6439
13. Zhao, M., Morohashi, K., Hatlestad, G., Grotewold, E., and Lloyd, A. (2008) The TTG1-bHLH-MYB complex controls trichome cell fate and patterning through direct targeting of regulatory loci. *Development* **135,** 1991–1999
14. Zhang, F., Gonzalez, A., Zhao, M., Payne, C. T., and Lloyd, A. (2003) A network of redundant bHLH proteins functions in all TTG1-dependent pathways of *Arabidopsis*. *Development* **130,** 4859–4869
15. Payne, C. T., Zhang, F., and Lloyd, A. M. (2000) GL3 encodes a bHLH protein that regulates trichome development in *Arabidopsis* through interaction with GL1 and TTG1. *Genetics* **156,** 1349–1362
16. Di Cristina, M., Sessa, G., Dolan, L., Linstead, P., Baima, S., Ruberti, I., and Morelli, G. (1996) The *Arabidopsis* Athb-10 (GLABRA2) is an HD-Zip protein required for regulation of root hair development. *Plant J.* **10,** 393–402
17. Rerie, W. G., Feldmann, K. A., and Marks, M. D. (1994) The GLABRA2 gene encodes a homeo domain protein required for normal trichome development in *Arabidopsis*. *Genes Dev.* **8,** 1388–1399
18. Ohashi, Y., Oka, A., Ruberti, I., Morelli, G., and Aoyama, T. (2002) Entopically additive expression of GLABRA2 alters the frequency and spacing of trichome initiation. *Plant J.* **29,** 359–369
19. Szymanski, D. B., Jilk, R. A., Pollock, S. M., and Marks, M. D. (1998) Control of GL2 expression in *Arabidopsis* leaves and trichomes. *Development* **125,** 1161–1171
20. Morohashi, K., and Grotewold, E. (2009) A systems approach reveals regulatory circuitry for *Arabidopsis* trichome initiation by the GL3 and GL1 selectors. *PLoS Genet.* **5,** e1000396
21. Wada, T., Tachibana, T., Shimura, Y., and Okada, K. (1997) Epidermal cell differentiation in *Arabidopsis* determined by a Myb homolog, CPC. *Science* **277,** 1113–1116
22. Wada, T., Kurata, T., Tominaga, R., Koshino-Kimura, Y., Tachibana, T., Goto, K., Marks, M. D., Shimura, Y., and Okada, K. (2002) Role of a positive regulator of root hair development, CAPRICE, in *Arabidopsis* root epidermal cell differentiation. *Development* **129,** 5409–5419
23. Schellmann, S., Schnittger, A., Kirik, V., Wada, T., Okada, K., Beermann, A., Thumfahrt, J., Jürgens, G., and Hülskamp, M. (2002) TRIPTYCHON and CAPRICE mediate lateral inhibition during trichome and root hair patterning in *Arabidopsis*. *EMBO J.* **21,** 5036–5046
24. Esch, J. J., Chen, M. A., Hillestad, M., and Marks, M. D. (2004) Comparison of TRY and the closely related At1g01380 gene in controlling *Arabidopsis* trichome patterning. *Plant J.* **40,** 860–869
25. Kirik, V., Simon, M., Huelskamp, M., and Schiefelbein, J. (2004) The ENHANCER OF TRY AND CPC1 gene acts redundantly with TRIPTYCHON and CAPRICE in trichome and root hair cell patterning in *Arabidopsis*. *Dev. Biol.* **268,** 506–513
26. Kirik, V., Simon, M., Wester, K., Schiefelbein, J., and Hulskamp, M. (2004) ENHANCER of TRY and CPC 2 (ETC2) reveals redundancy in the region-specific control of trichome development of *Arabidopsis*. *Plant Mol. Biol.* **55,** 389–398
27. Simon, M., Lee, M. M., Lin, Y., Gish, L., and Schiefelbein, J. (2007) Distinct and overlapping roles of single-repeat MYB genes in root epidermal patterning. *Dev. Biol.* **311,** 566–578
28. Tominaga, R., Iwata, M., Sano, R., Inoue, K., Okada, K., and Wada, T. (2008) *Arabidopsis* CAPRICE-LIKE MYB 3 (CPL3) controls endoreduplication and flowering development in addition to trichome and root hair formation. *Development* **135,** 1335–1345
29. Wang, S., Hubbard, L., Chang, Y., Guo, J., Schiefelbein, J., and Chen, J. G. (2008) Comprehensive analysis of single-repeat R3 MYB proteins in epidermal cell patterning and their transcriptional regulation in *Arabidopsis*. *BMC Plant Biol.* **8,** 81
30. Digiuni, S., Schellmann, S., Geier, F., Greese, B., Pesch, M., Wester, K., Dartan, B., Mach, V., Srinivas, B. P., Timmer, J., Fleck, C., and Hulskamp, M. (2008) A competitive complex formation mechanism underlies trichome patterning on *Arabidopsis* leaves. *Mol. Syst. Biol.* **4,** 217
31. Wester, K., Digiuni, S., Geier, F., Timmer, J., Fleck, C., and Hülskamp, M. (2009) Functional diversity of R3 single-repeat genes in trichome development. *Development* **136,** 1487–1496
32. Larkin, J. C., Oppenheimer, D. G., Lloyd, A. M., Paparozzi, E. T., and Marks, M. D. (1994) Roles of the GLABROUS1 and TRANSPARENT TESTA GLABRA Genes in *Arabidopsis* Trichome Development. *Plant Cell* **6,** 1065–1076
33. Stracke, R., Werber, M., and Weisshaar, B. (2001) The R2R3-MYB gene family in *Arabidopsis thaliana*. *Curr. Opin. Plant Biol.* **4,** 447–456
34. Kirik, V., Lee, M. M., Wester, K., Herrmann, U., Zheng, Z., Oppenheimer, D., Schiefelbein, J., and Hulskamp, M. (2005) Functional diversification of MYB23 and GL1 genes in trichome morphogenesis and initiation. *Development* **132,** 1477–1485
35. Esch, J. J., Chen, M., Sanders, M., Hillestad, M., Ndkium, S., Idelkope, B., Neizer, J., and Marks, M. D. (2003) A contradictory GLABRA3 allele helps define gene interactions controlling trichome development in *Arabidopsis*. *Development* **130,** 5885–5894
36. Feller, A., Hernandez, J. M., and Grotewold, E. (2006) An ACT-like domain participates in the dimerization of several plant basic-helix-loop-helix transcription factors. *J. Biol. Chem.* **281,** 28964–28974
37. Heim, M. A., Jakoby, M., Werber, M., Martin, C., Weisshaar, B., and Bailey, P. C. (2003) The basic helix-loop-helix transcription factor family in plants. A genome-wide study of protein structure and functional diversity. *Mol. Biol. Evol.* **20,** 735–747
38. Toledo-Ortiz, G., Huq, E., and Quail, P. H. (2003) The *Arabidopsis* basic/helix-loop-helix transcription factor family. *Plant Cell* **15,** 1749–1770
39. Baudry, A., Heim, M. A., Dubreucq, B., Caboche, M., Weisshaar, B., and Lepiniec, L. (2004) TT2, TT8, and TTG1 synergistically specify the ex-

pression of BANYULS and proanthocyanidin biosynthesis in *Arabidopsis thaliana*. *Plant J.* **39,** 366–380
40. Nesi, N., Debeaujon, I., Jond, C., Pelletier, G., Caboche, M., and Lepiniec, L. (2000) The TT8 gene encodes a basic helix-loop-helix domain protein required for expression of DFR and BAN genes in *Arabidopsis* siliques. *Plant Cell* **12,** 1863–1878
41. Baudry, A., Caboche, M., and Lepiniec, L. (2006) TT8 controls its own expression in a feedback regulation involving TTG1 and homologous MYB and bHLH factors, allowing a strong and cell-specific accumulation of flavonoids in *Arabidopsis thaliana*. *Plant J.* **46,** 768–779
42. Cone, K. C., Burr, F. A., and Burr, B. (1986) Molecular analysis of the maize anthocyanin regulatory locus C1. *Proc. Natl. Acad. Sci. U.S.A.* **83,** 9631–9635
43. Goff, S. A., Cone, K. C., and Chandler, V. L. (1992) Functional analysis of the transcriptional activator encoded by the maize B gene. Evidence for a direct functional interaction between two classes of regulatory proteins. *Genes Dev.* **6,** 864–875
44. Urao, T., Yamaguchi-Shinozaki, K., Mitsukawa, N., Shibata, D., and Shinozaki, K. (1996) Molecular cloning and characterization of a gene that encodes a MYC-related protein in *Arabidopsis*. *Plant Mol. Biol.* **32,** 571–576
45. Zimmermann, I. M., Heim, M. A., Weisshaar, B., and Uhrig, J. F. (2004) Comprehensive identification of *Arabidopsis thaliana* MYB transcription factors interacting with R/B-like BHLH proteins. *Plant J.* **40,** 22–34
46. Symonds, V. V., Hatlestad, G., and Lloyd, A. M. (2011) Natural allelic variation defines a role for ATMYC1. Trichome cell fate determination. *PLoS Genetics* **7,** e1002069
47. Lukowitz, W., Gillmor, C. S., and Scheible, W. R. (2000) Positional cloning in *Arabidopsis*. Why it feels good to have a genome initiative working for you. *Plant Physiol.* **123,** 795–805
48. Wang, Z., Yuan, T., Yuan, C., Niu, Y., Sun, D., and Cui, S. (2009) LFR, which encodes a novel nuclear-localized Armadillo-repeat protein, affects multiple developmental processes in the aerial organs in *Arabidopsis*. *Plant Mol. Biol.* **69,** 121–131
49. Clough, S. J., and Bent, A. F. (1998) Floral dip. A simplified method for *Agrobacterium*-mediated transformation of *Arabidopsis thaliana*. *Plant J.* **16,** 735–743
50. Cao, Y., Dai, Y., Cui, S., and Ma, L. (2008) Histone H2B monoubiquitination in the chromatin of FLOWERING LOCUS C regulates flowering time in *Arabidopsis*. *Plant Cell* **20,** 2586–2602
51. Walter, M., Chaban, C., Schütze, K., Batistic, O., Weckermann, K., Näke, C., Blazevic, D., Grefen, C., Schumacher, K., Oecking, C., Harter, K., and Kudla, J. (2004) Visualization of protein interactions in living plant cells using bimolecular fluorescence complementation. *Plant J.* **40,** 428–438
52. Asai, T., Tena, G., Plotnikova, J., Willmann, M. R., Chiu, W. L., Gomez-Gomez, L., Boller, T., Ausubel, F. M., and Sheen, J. (2002) MAP kinase signaling cascade in *Arabidopsis* innate immunity. *Nature* **415,** 977–983
53. Morohashi, K., Zhao, M., Yang, M., Read, B., Lloyd, A., Lamb, R., and Grotewold, E. (2007) Participation of the *Arabidopsis* bHLH factor GL3 in trichome initiation regulatory events. *Plant Physiol.* **145,** 736–746
54. Yoshida, Y., Sano, R., Wada, T., Takabayashi, J., and Okada, K. (2009) Jasmonic acid control of GLABRA3 links inducible defense and trichome patterning in *Arabidopsis*. *Development* **136,** 1039–1048
55. Bernhardt, C., Zhao, M., Gonzalez, A., Lloyd, A., and Schiefelbein, J. (2005) The bHLH genes GL3 and EGL3 participate in an intercellular regulatory circuit that controls cell patterning in the *Arabidopsis* root epidermis. *Development* **132,** 291–298
56. Lee, M. M., and Schiefelbein, J. (2001) Developmentally distinct MYB genes encode functionally equivalent proteins in *Arabidopsis*. *Development* **128,** 1539–1546
57. Coletta, A., Pinney, J. W., Solís, D. Y., Marsh, J., Pettifer, S. R., and Attwood, T. K. (2010) Low complexity regions within protein sequences have position-dependent roles. *BMC Syst. Biol.* **4,** 43
58. Maes, L., Inzé, D., and Goossens, A. (2008) Functional specialization of the TRANSPARENT TESTA GLABRA1 network allows differential hormonal control of laminal and marginal trichome initiation in *Arabidopsis* rosette leaves. *Plant Physiol.* **148,** 1453–1464
59. Gallet, X., Charloteaux, B., Thomas, A., and Brasseur, R. (2000) A fast method to predict protein interaction sites from sequences. *J. Mol. Biol.* **302,** 917–926